JACS
JOURNAL OF THE AMERICAN CHEMICAL SOCIETY

ARTICLE

pubs.acs.org/JACS

Reversible Cross-Linking of Polyisoprene Coronas in Micelles, Block Comicelles, and Hierarchical Micelle Architectures Using Pt(0)−Olefin Coordination

Paul A. Rupar,[†] Graeme Cambridge,[‡] Mitchell A. Winnik,*[,‡] and Ian Manners*[,†]

[†]School of Chemistry, University of Bristol, Bristol, United Kingdom, BS8 1TS

[‡]Department of Chemistry, University of Toronto, Toronto, Ontario, Canada, M5S 3H6

Supporting Information

ABSTRACT: Previous work has established that polyisoprene (PI) coronas in cylindrical block copolymer micelles with a poly(ferrocenyldimethylsilane) (PFS) core can be irreversibly cross-linked by hydrosilylation using $(HSiMe_2)_2O$ in the presence of Karstedt's catalyst. We now show that treatment of cylindrical PI-*b*-PFS micelles with Karstedt's catalyst alone, in the absence of any silanes, leads to PI coronal cross-linking through Pt(0)−olefin coordination. The cross-linking can be reversed through the addition of 2-bis(diphenylphosphino)-ethane (dppe), a strong bidentate ligand, which removes the platinum from the PI to form $Pt(dppe)_2$. The Pt(0) cross-linking of PI was studied with self-assembled cylindrical PI-*b*-PFS block copolymer micelles, where the cross-linking was found to dramatically increase the stability of the micellar structures. The Pt(0)−alkene coordination-induced cross-linking can be used to provide transmission electron microscopy contrast between PI and poly(dimethylsiloxane) (PDMS) corona domains in block comicelles as the process selectively increases the electron density of the PI regions. Moreover, following the assembly of a hierarchical scarf-shaped comicelle consisting of a PFS-*b*-PDMS platelet template with PI-*b*-PFS tassels, Pt(0)-induced cross-linking of the PI coronal regions allowed for the selective removal of the PFS-*b*-PDMS center, leaving behind an unprecedented hollowed-out scarf structure. The addition of Karstedt's catalyst to PI or polybutadiene homopolymer toluene/xylene solutions resulted in the formation of polymer gels which underwent de-gelation upon the addition of dppe.

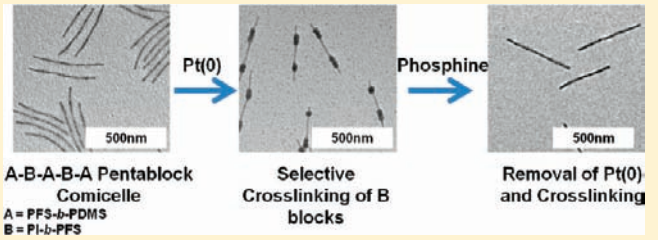

INTRODUCTION

Block copolymers (BCPs) can self-assemble into micellar structures consisting of solvent-swollen coronas and solvent-insoluble cores when placed in a solvent selective for only one of the blocks.[1] By varying the BCP composition, solvent conditions, concentration, and temperature, a range of micelle morphologies are possible.[1b,2] Ease of formation and morphological diversity make BCP micelles among the most promising soft matter nanomaterials with potential applications in targeted drug delivery,[3] as etch resists,[4] in solution templating of inorganic materials,[5] as ceramic precursors,[6] and in composite reinforcement.[7]

Unfortunately, the potentially dynamic nature of BCP micelles can hinder their use in applications. Although the critical micelle concentration (CMC) of polymer micelles is much lower than that of small-molecule surfactants, BCP micelles are still susceptible to disassembly in high dilution.[1a,b] Changes in solvent conditions, increases in temperature, and mechanical stress and shear forces can also rapidly degrade micellar structures. These considerations have motivated important breakthroughs in the stabilization of BCP micelles through the cross-linking of either the corona or core of the structure.[8,9] Cross-linking freezes micelle structures via interchain bonding, thereby increasing the robustness of the self-assembled nanostructure and effectively enhancing their potential utility. A wide variety of micelle cross-linking methodologies have been developed, which include radical-induced bond formation,[8a,10] photo-induced cycloadditions,[8d,11] siloxane condensation,[12] the use of bifunctional linking agents,[8b,13] and many others.[9] BCP micelles with reversible cross-linking, such as those containing redox-reversible disulfide bonds,[14] are of particular interest because they introduce additional versatility and an element of stimulus responsivity.[9] However, homopolymers and block copolymers that exhibit reversible cross-linking are generally purposely designed with specific functional groups; simple, commodity polymers (such as polyisoprene, PI) can be difficult to reversibly cross-link due to their limited chemical functionality.

The introduction of metal centers to block copolymers can lead to additional opportunities for applications as functional materials.[15] We have been particularly interested in the solution self-assembly behavior of BCPs with a semicrystalline poly(ferrocenyldimethylsilane) (PFS) metalloblock. When the PFS block is short, BCPs such as PI-*b*-PFS and PFS-*b*-poly(dimethylsiloxane) (PFS-*b*-PDMS) (Chart 1) preferentially

Received: July 9, 2011
Published: October 03, 2011

Chart 1. Structures of PI-*b*-PFS and PFS-*b*-PDMS Diblock Copolymers Prepared by Sequential Anionic Polymerization

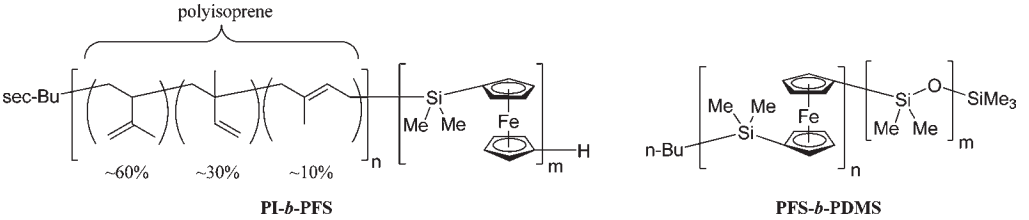

Scheme 1. Bidirectional Cylindrical Micelle Growth through the Epitaxy of PFS-Containing BCPs from PFS-*b*-PDMS Micelles with a Crystalline PFS Core (Yellow = PFS, Red = PDMS, Blue = PI)

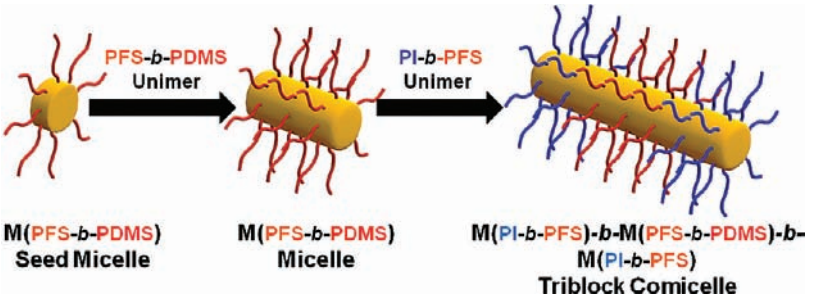

form cylindrical micelles with a crystalline PFS core in a solvent selective for the complementary block.[16] The crystallization of the core-forming PFS block drives the formation of the cylindrical structures, which arise as a compromise between the preference of the crystalline PFS block to form sheet-like platelets and the steric repulsion of the corona chains which promotes curvature of the core−corona interface.[16a,17]

Remarkably, the contour length of PFS-containing BCP cylindrical micelles can be increased in a controlled and predictable manner by the addition of further PFS BCP unimer to a solution of preexisting cylinders.[18,19] The exposed crystalline PFS cores of the preformed cylinders incorporate new unimers by acting as nucleation sites for the epitaxial crystallization of the PFS block of the added PFS BCP unimers. This crystallization-driven self-assembly is a living process, as the cylinder ends remain indefinitely active to the integration of new PFS BCP molecules. PFS BCPs with different corona-forming blocks can also be incorporated into preformed micelles via epitaxy, resulting in the creation of block comicelles featuring chemically distinct corona segments (Scheme 1). We have employed this crystallization-driven living self-assembly process to form micelles with a narrow length distribution (PDI ≤ 1.03) by utilizing short PFS-*b*-PDMS seed micelles as initiators for the self-assembly of longer cylinders (Scheme 1).[20] Recently it has emerged that BCPs containing semicrystalline poly(ferrocenyldiethylsilane),[21] poly(lactide),[22] or poly(3-hexylthiophene)[23] blocks also undergo cylindrical micelle lengthening, suggesting the operation of a similar epitaxial growth process.

We have previously studied the corona cross-linking of PI-*b*-PFS and PFS-*b*-poly(methylvinylsiloxane) (PFS-*b*-PMVS) cylindrical micelles through the Pt(0)-promoted hydrosilylation of 1,1,3,3-tetramethyldisiloxane (TMDS).[24] Corona cross-linking was found to greatly increase the stability of the micelles, allowing structure retention in good solvents for both blocks and during exposure to ultrasound. Partially oxidized cross-linked PFS-*b*-PMVS micelles have been found to template "peapod" Ag nanowires within the micelle core,[24b] and cross-linked PI-*b*-PFS cylindrical micelles template magnetic ceramic materials containing arrays of Fe nanoparticles through a pyrolysis procedure.[24c,d] Cross-linked PFS BCP micelles have also been used in microfluidic channel-assisted nanopatterning.[24c,d]

Chart 2. Structure of Karstedt's Catalyst Based on X-ray Crystallographic Analysis[27c]

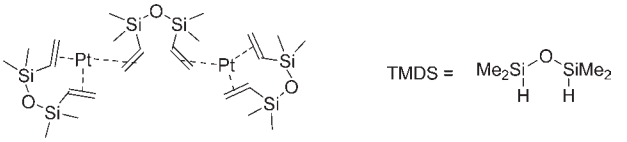

In this report we return to the cross-linking of PI-*b*-PFS micelles, where we now demonstrate the cross-linking of PI through Pt(0)−olefin coordination. We have discovered that the cross-linking can occur in the absence of a bifunctional silane and can be reversed through the addition of a chelating phosphine ligand. When applied to PI-*b*-PFS micelles and PI-*b*-PFS-containing block comicelles, Pt(0)−alkene coordination within the PI corona permits the micelles to remain stable in a good solvent for both PI and PFS, hinders micelle degradation during sonication, and increases the contrast of the PI corona in TEM micrographs. We exploit the selectivity of Pt(0) centers to cross-link PI by removing the PFS-*b*-PDMS template from a cross-linked PI-*b*-PFS hierarchical scarf-like micelle structure. The cross-linking can also be applied to PI and polybutadiene (PB) homopolymer, where the reversible formation of polymer gels is observed in solution.

RESULTS AND DISCUSSION

1. Corona Cross-Linking of Cylindrical PI-*b*-PFS Micelles via Reversible Pt(0) Coordination. Following the first report in

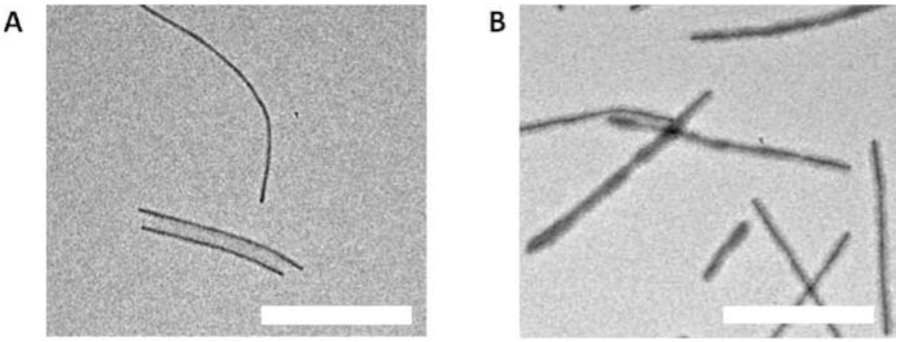

Figure 1. (A) TEM micrograph of PI_{637}-*b*-PFS_{53} micelles. (B) TEM micrograph of PI_{637}-*b*-PFS_{53} micelles cross-linked with TMDS using 10 mol % Karstedt's catalyst. Scale bars are 500 nm.

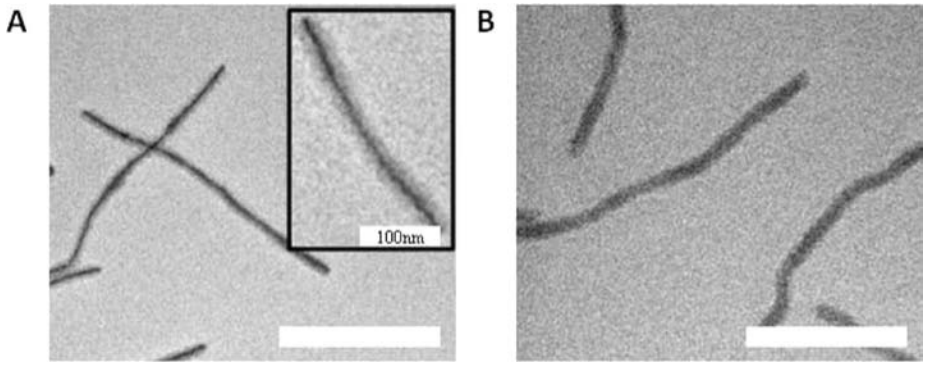

Figure 2. (A) TEM micrograph of PI_{637}-*b*-PFS_{53} cylindrical micelles after addition of Karstedt's catalyst (10 mol % Pt/olefin). In the inset image, the darkened PI corona is easily distinguished from the thinner dark line attributed to the crystalline PFS core. (B) TEM micrograph of PI_{637}-*b*-PFS_{53} cylindrical micelles after addition of Karstedt's catalyst and cast from a THF solution. Scale bars are 500 nm unless noted otherwise.

the patent literature,[25] Karstedt's catalyst was developed as a highly active hydrosilylation catalyst formed from the reaction of Speier's catalyst (H_2PtCl_6) with 1,3-divinyltetramethyldisiloxane.[26] With a structure consisting of Pt(0) centers coordinated by vinyl siloxanes (Chart 2), the labile nature of the siloxane ligands is thought to be responsible for the high catalytic activity of Karstedt's catalyst.[27]

In previous studies, PI-*b*-PFS cylindrical micelles were cross-linked via Karstedt's catalyst-promoted hydrosilylation with TMDS. Reactions were performed with low catalyst loading, typically around 0.1 mol % relative to PI repeat units, and occurred over several days.[24c,d] To shorten the reaction time, TMDS cross-linking of PI_{637}-*b*-PFS_{53} micelles was attempted with 10 mol % Karstedt's catalyst, a 100 times increase in catalyst loading compared to our previous work. As desired, the time necessary to cross-link the micelles was decreased to 18 h. A comparison of transmission electron microscopy (TEM) micrographs of the PI_{637}-*b*-PFS_{53} micelles before (Figure 1A) and after cross-linking (Figure 1B) shows an apparent darkening of the PI corona after the cross-linking procedure. Energy-dispersive X-ray spectroscopy (EDX) of the sample produced signals attributable to Pt (see Supporting Information, Figure S1). The detection of platinum by EDX was surprising, given that the micelle solution was passed through a short alumina column with the intent to remove residual Pt prior to TEM and EDX analysis.

We hypothesized that the residual platinum detected by EDX and the concurrent darkening of the PI_{637}-*b*-PFS_{53} micelles in the TEM micrograph was due to the formation of Pt(0) complexes within the PI corona. As the vinyl siloxane ligands of Karstedt's catalyst are labile,[27a] this suggested that the Pt(0) ligands could have been displaced by the PI vinyl groups, a process assisted by the high local concentration of alkene groups within the micelle corona. Homoleptic Pt(0)−olefin complexes are often tricoordinate (e.g., Pt(2-norbornene)$_3$ and Pt$(CH_2CH_2)_3$), although tetra-olefin complexation is also possible (e.g., Pt(1,5-cyclooctadiene)$_2$).[28] Therefore, if Pt(0)−olefin bonds form within the PI corona, the Pt centers could bridge multiple polymer chains within individual micelles and TMDS would not be necessary to establish cross-linking.

The cross-linking experiment with a high catalyst loading was repeated with the exclusion of TMDS to determine if Karstedt's catalyst was interacting with the micelles. Karstedt's catalyst (10 mol % Pt/olefin) was added to a hexane solution of cylindrical PI_{637}-*b*-PFS_{53} micelles. Compared to TEM micrographs of PI_{637}-*b*-PFS_{53} micelles prior to any manipulations (Figure 1A), the corona of the micelles after addition of Karstedt's catalyst displayed higher contrast (Figure 2A), and EDX line analysis showed the presence of platinum localized on the cylinders (see Supporting Information, Figure S2). To determine if the micelles were cross-linked by Karstedt's catalyst, the micelles were transferred to THF, a good solvent for both PI and PFS which, in the absence of cross-linking, causes PI-*b*-PFS-based micelles to rapidly disassemble to form unimers. However, after exposure to Karstedt's catalyst, THF-dispersed cylindrical PI_{637}-*b*-PFS_{53} micelles remained clearly intact in the TEM micrographs, suggesting that the micelles are indeed cross-linked

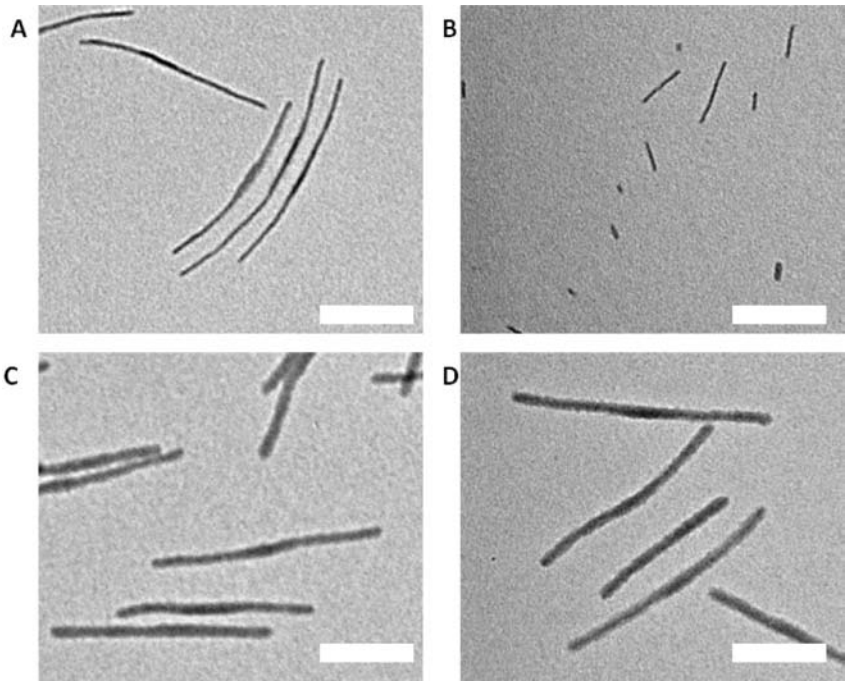

Figure 3. (A) TEM micrograph of PI_{637}-*b*-PFS_{53} cylindrical micelles with an average contour length of 530 nm. (B) TEM micrograph of non-cross-linked PI_{637}-*b*-PFS_{53} micelles after undergoing ultrasonication treatment for 10 min. (C) TEM micrograph of Pt(0) cross-linked 530 nm PI_{637}-*b*-PFS_{53} cylindrical micelles. (D) TEM micrograph of Pt(0) cross-linked 530 nm PI_{637}-*b*-PFS_{53} cylindrical micelles after undergoing ultrasonication treatment for 10 min. Scale bars are 250 nm.

Table 1. Comparison of Average Micelle Contour Lengths (L_n), PDI, and RSD before Sonication, after Sonication, and after Cross-Linking followed by Sonication

entry	description	no. of micelles measured (N)	L_n (nm)	PDI	RSD (σ/L_n)
1	PI_{637}-*b*-PFS_{53} micelles before sonication	423	526[a]	1.03[a]	0.18[a]
2	PI_{637}-*b*-PFS_{53} micelles after sonication	413	93	1.31	0.56
3	Pt(0) cross-linked PI_{637}-*b*-PFS_{53} micelles before sonication	406	568[a]	1.02[a]	0.15[a]
4	Pt(0) cross-linked PI_{637}-*b*-PFS_{53} micelles after sonication	317	536	1.06	0.25

[a] The L_n, PDI, and RSD of PI_{637}-*b*-PFS_{53} micelles in entries 1 and 3 should be identical before and after cross-linking. The variation between samples 1 and 3 may be a consequence of the fact that the contour length of sample 3 includes contributions from the now visible cross-linked PI corona. See Figure 3A,C.

(Figure 2B). TEM micrographs of the cylinders cast from THF solution appear swollen compared to micelles cast from the selective solvent hexane, a behavior that has been previously observed with PI-*b*-PFS micelles cross-linked via hydrosilylation.[24c,d]

The evidence for micelle cross-linking was further strengthened through an examination of the mechanical stability of the micelles. Non-cross-linked PFS block copolymer micelles exposed to ultrasound have been shown to fracture into smaller cylindrical structures, whereas cross-linked micelles were left unaltered.[16b,18,20,24d,29] First, we created a batch of cylindrical PI_{637}-*b*-PFS_{53} micelles in decane with an average contour length (L_n) of about 530 nm using a temperature-controlled self-seeding process (see Supporting Information, Scheme S1).[30] The self-seeded micelles had a narrow length distribution, as illustrated by a polydispersity index (PDI) of 1.03 and a low relative standard deviation (RSD) of 0.18 (Figure 3A and Table1, entry 1). The monodisperse micelle solution in decane was split in half, and 10 mol % Karstedt's catalyst was added to one of the subdivided micelle solutions. Both PI_{637}-*b*-PFS_{53} micelle solutions, one non-cross-linked and one cross-linked with Pt(0), were then placed in a 160 W ultrasonic bath for 10 min. TEM micrographs of the original, non-cross-linked PI_{637}-*b*-PFS_{53} micelles after sonication showed a dramatic change in length and length distribution (Figure 3B and Table 1, entry 2). The micelles were much smaller (L_n = 93 nm), and the PDI increased to 1.31 and the RSD to 0.56 (Table 1, entry 2). In contrast, TEM micrographs of the cross-linked micelles showed little change. The L_n of the cross-linked micelles remained almost constant, while the PDI and RSD increased only slightly to 1.06 and 0.25, respectively (Figure 3D and Table 1, entry 4). Examination of the micelle solutions by dynamic light scattering (DLS) also showed that the apparent hydrodynamic radius ($R_{H,app}$) of the non-cross-linked micelles decreased during ultrasonication, while the $R_{H,app}$ of the cross-linked micelles was unchanged (see Supporting Information, Figure S9 and Table S2). The decrease in $R_{H,app}$ observed with the non-cross-linked micelles under ultrasonication is consistent with the fragmentation of the cylindrical micelles visualized by TEM (Figure 3B). The results from these experiments

Chart 3. Possible Pt(0) Coordination in the PI Corona (Only PI Vinyl Groups Are Shown for Simplicity)

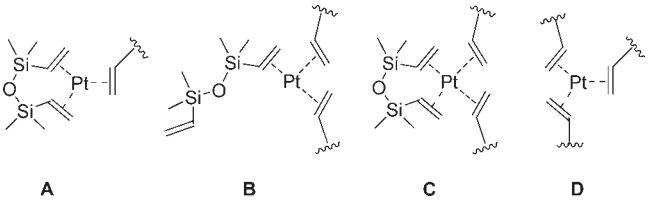

are clearly consistent with cross-linking of the PI_{637}-*b*-PFS_{53} micelles by Karstedt's catalyst in the absence of TMDS.

In order to further support that Pt(0)−vinyl complexation was responsible for the micelle cross-linking, we attempted to cross-link cylindrical PFS_{60}-*b*-$PDMS_{660}$ micelles, where the corona is devoid of alkenes, using Karstedt's catalyst. In a series of experiments, we varied the amount of Pt(0) catalyst added to cylindrical PFS_{60}-*b*-$PDMS_{660}$ micelles in hexane. Darkening of the PDMS corona was not apparent in the TEM micrographs of the PFS_{60}-*b*-$PDMS_{660}$ micelles exposed to Karstedt's catalyst (see Supporting Information, Scheme S2). Furthermore, when cylindrical PFS_{60}-*b*-$PDMS_{660}$ micelles in the presence of Karstedt's catalyst were dispersed in THF (a good solvent for both PFS and PDMS), the micelles were no longer observed in TEM micrographs, which was consistent with the disassembly of the PFS_{60}-*b*-$PDMS_{660}$ micelles into unimers. Finally, PFS_{60}-*b*-$PDMS_{660}$ micelles exposed to Karstedt's catalyst were observed to have decreased contour lengths upon sonication (see Supporting Information, Scheme S2). All of these observations strongly indicated that the PFS_{60}-*b*-$PDMS_{660}$ cylindrical micelles were not cross-linked by Karstedt's catalyst and that cross-linking of the PI_{637}-*b*-PFS_{53} micelles is associated with the PI corona and not the PFS core of the micelle.

The previous experiments are consistent with cross-linking that occurs through coordination of corona PI alkene groups to Pt(0). In general, platinum-bound olefins are labile and easily undergo substitution.[31] Although the vinyl siloxane ligands of Karstedt's catalyst represent relatively strongly bound olefins,[32] examples of alkene exchanges through vinyl siloxane substitution are known.[27a,c,33] The high concentration of alkene groups within the PI corona of the micelles would provide a strong driving force for PI coordination of platinum through the displacement of the vinyl siloxane ligands. Assuming that the bridged dinuclear complex depicted in Chart 2 is the primary species in a solution of Karstedt's catalyst,[27c] a number of Pt(0)−PI coordination configurations can be envisioned (Chart 3). In the first instance, a PI alkene could displace the bridging siloxane ligand to form **A**, although this configuration could not induce polymer interchain cross-linking. In **B**, two PI olefins coordinate through the loss of one divinyldisiloxane and the monodentate coordination of another. Configuration **C** is a possible 18-electron platinum complex formed from two PI alkenes and a single bidentate divinyldisiloxane ligand. Finally, in **D**, all of the siloxane ligands are displaced, and three PI olefins coordinate the platinum center. An 18-electron version of **D** with four PI vinyl groups is also possible. Depending on the local environment within the micelle corona, it is plausible that a combination of **A**−**D** forms upon addition of Karstedt's catalyst to PI_{637}-*b*-PFS_{53} micelles.

If our hypothesis is correct—that Pt(0)−olefin coordination is responsible for the cross-linking of the PI_{637}-*b*-PFS_{53} micelles—the addition of a stronger ligand, such as a phosphine, should displace the olefins bound to platinum and reverse the cross-linking. When 2-bis(diphenylphosphino)ethane (dppe) was added to a solution of Pt(0)-cross-linked PI_{637}-*b*-PFS_{53} micelles, a bright yellow solution formed. ^{31}P NMR spectroscopy of the solution showed $Pt(dppe)_2$ as the only new phosphorus-containing compound (see Supporting Information, Figure S5).[34] After reaction with dppe, the Pt-induced darkening in TEM micrographs was no longer observable, and Pt was no longer detected by EDX analysis. Furthermore, the PI_{637}-*b*-PFS_{53} micelles were no longer stable in the common solvent THF, which is consistent with the reversal of the PI cross-linking. ^{1}H NMR spectroscopy of Pt-cross-linked micelles purified through centrifugation, resuspended in C_6D_6, and subsequently reacted with dppe showed weak signals attributable to 1,3-divinyltetramethyldisiloxane (see Supporting Information, Figure S8). We suspect that some divinyldisiloxane ligands remain bound to the platinum during PI coordination as depicted in Chart 3, **A**−**C**, and are only released upon dppe addition. ^{1}H NMR spectra and GPC traces of the PI_{637}-*b*-PFS_{53} block copolymer before and after Pt coordination were identical within experimental error, which indicated that the polymer is essentially unaltered by the reversible cross-linking process (see Supporting Information, Figures S3, S4, and S6).

Attempts at observing a ^{195}Pt NMR signal associated with the cross-linked micelles have not been successful; this, however, is not surprising given that simple Pt(0) olefin complexes can give multiple signals due to rapid ligand dissociation.[35] We do not believe that nanoparticles (NPs) are acting as the cross-linking agent,[36] as we have been unable to visualize Pt-NPs by TEM or detect NPs by UV−vis spectroscopy (see Supporting Information, Figure S7).

The addition of dppe to PI_{637}-*b*-PFS_{53} micelles cross-linked by Karstedt's catalyst-promoted hydrosilylation with TMDS does result in the formation of a small amount of $Pt(dppe)_2$. However, the TMDS cross-linked PI_{637}-*b*-PFS_{53} micelles retain structural stability in THF even after the addition of dppe, indicating that irreversible TMDS-bridged cross-linking is present. We therefore conclude that, under the conditions used in our previous cross-linking studies (low catalyst loading in the presence of TMDS),[24] the primary cross-linking mechanism is hydrosilylation with TMDS and not Pt(0)−olefin interactions. Only at higher loadings of Karstedt's catalyst, in the absence of TMDS, does Pt(0)−olefin coordination become the primary cross-linking mechanism in PI-*b*-PFS micelles.[37]

2. Selective Cross-Linking and Staining of PI Coronas in Cylindrical Block Comicelles. Since most polymers are composed of low atomic number elements, examining BCP micelles via TEM can be difficult due to poor contrast. PFS BCP micelles are an exception, as the electron-rich PFS cores provide good contrast in TEM micrographs (e.g., Figures 1A and 3A), although differentiation between different coronal domains remains a challenge.[18] To help visualize polymers in TEM micrographs, heavy transition-metal-based compounds with specific functional group reactivity can be used as staining agents.[38] For example, OsO_4 reacts with C=C bonds and is often used to selectively stain diene polymers such as PI. However, OsO_4 is very toxic, requires careful handling techniques, and is expensive.[38] We envision that Karstedt's catalyst can be used as an alternative to traditional staining methods for polymers containing unsaturation. Karstedt's catalyst is less hazardous than volatile transition metal oxides, is available commercially as a xylenes solution, and

Scheme 2. Self-Assembly of a Pentablock Comicelle through Sequential Addition of PI_{637}-*b*-PFS_{53} and PFS_{60}-*b*-$PDMS_{660}$ Unimers to Short, Preformed PFS_{60}-*b*-$PDMS_{660}$ Cylindrical Micelle Seeds[a]

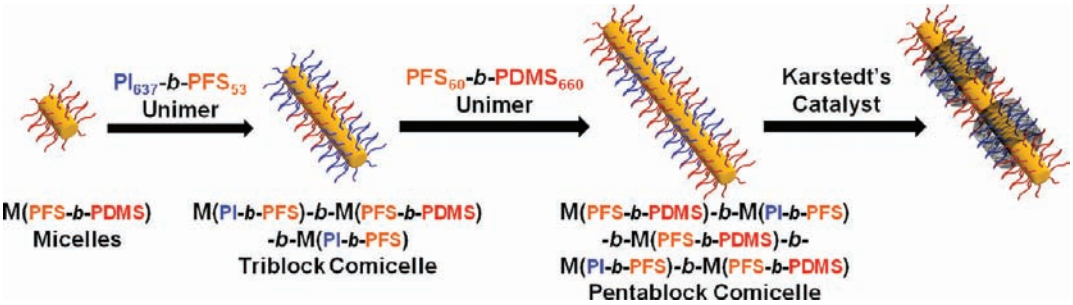

[a] The addition of Karstedt's catalyst selectively crosslinks the PI corona regions and provides contrast in TEM micrographs between the different comicelle blocks. For clarity, the degree of polymerization (DP_n) of the polymer blocks is omitted from the block comicelle nomenclature (yellow = PFS, red = PDMS, blue = PI).

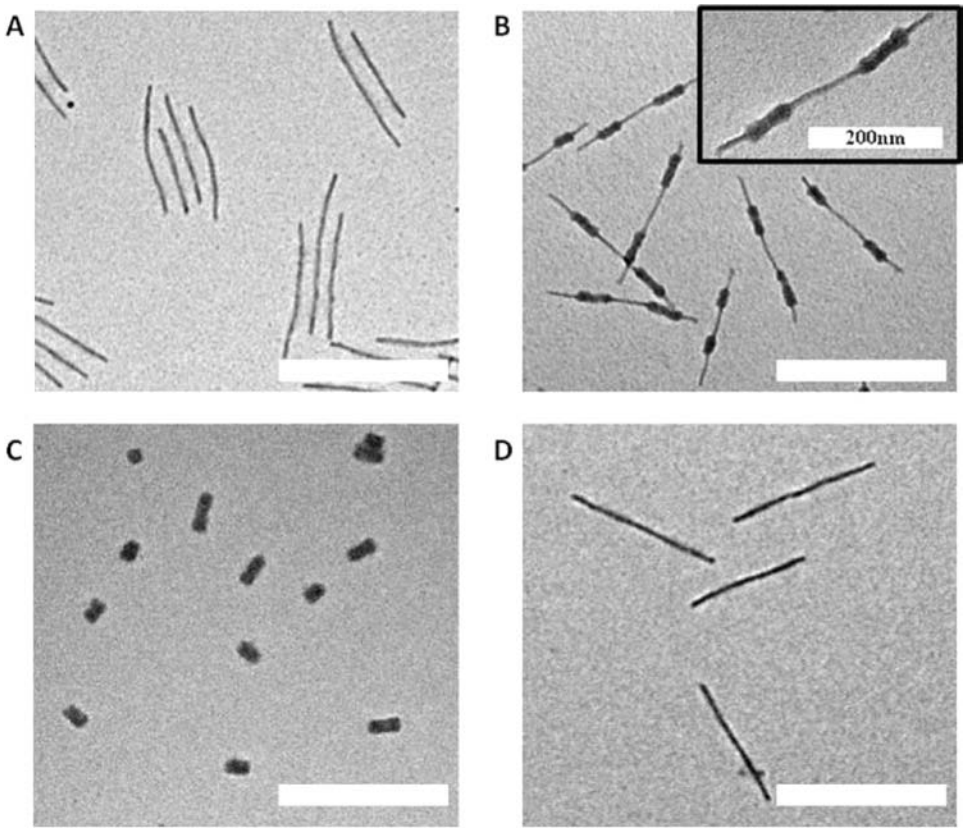

Figure 4. (A) M(PFS-*b*-PDMS)-*b*-M(PI-*b*-PFS)-*b*-M(PFS-*b*-PDMS)-*b*-M(PI-*b*-PFS)-*b*-M(PFS-*b*-PDMS) pentablock comicelles. (B) M(PFS-*b*-PDMS)-*b*-M(PI-*b*-PFS)-*b*-M(PFS-*b*-PDMS)-*b*-M(PI-*b*-PFS)-*b*-M(PFS-*b*-PDMS) block comicelles with the PI regions cross-linked by Pt(0) coordination. The darkened regions correspond to the Pt(0) cross-linked/stained PI corona blocks. (C) M(PFS-*b*-PDMS)-*b*-M(PI-*b*-PFS)-*b*-M(PFS-*b*-PDMS)-*b*-M(PI-*b*-PFS)-*b*-M(PFS-*b*-PDMS) pentablock comicelles with the PI regions cross-linked by Pt(0) coordination and then placed in THF. The PDMS regions have dissolved, leaving only the cross-linked PI regions intact. (D) Previously cross-linked M(PFS-*b*-PDMS)-*b*-M(PI-*b*-PFS)-*b*-M(PFS-*b*-PDMS)-*b*-M(PI-*b*-PFS)-*b*-M(PFS-*b*-PDMS) pentablock micelles after removal of Pt(0) with dppe. Scale bars are 500 nm unless noted otherwise.

can be delivered in solution very efficiently, requiring only very small amounts to achieve the desired staining effect.

To illustrate the selective staining capability of Karstedt's catalyst, pentablock comicelles with alternating PDMS and PI coronal domains were assembled by exploiting the ability of PFS BCP micelles to undergo controlled epitaxial growth.[18−20] PI_{637}-*b*-PFS_{53} unimers, followed by PFS_{60}-*b*-$PDMS_{660}$ unimers, were sequentially added to short, preformed PFS_{60}-*b*-$PDMS_{660}$ cylindrical micelle seeds to form pentablock comicelles with a sequential coronal composition of PDMS-PI-PDMS-PI-PDMS (Scheme 2 and Figure 4A). In the absence of staining, TEM micrographs of the pentablock comicelles displayed no contrast between the PI and PDMS coronal domains of the comicelles (Figure 4A). After Pt(0) cross-linking, TEM micrographs clearly

Scheme 3. Addition of PI_{637}-*b*-PFS_{53} Unimers to a Solution of PFS_{114}-*b*-$PDMS_{81}$ Platelets Results in the Growth of Tassels from the Platelets[a]

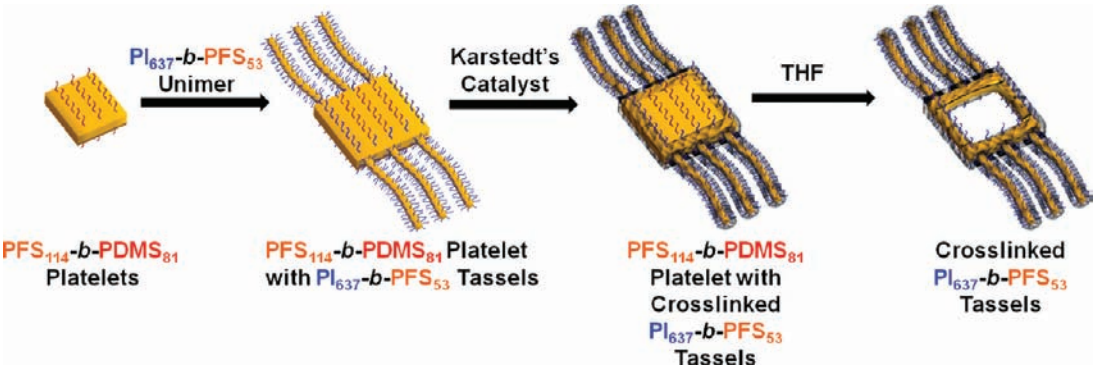

[a] Karstedt's catalyst selectively cross-links the PI_{637}-*b*-PFS_{53} domains. The non-cross-linked PFS_{114}-*b*-$PDMS_{81}$ regions dissolve in THF, leaving behind the cross-linked PI_{637}-*b*-PFS_{53} domains (yellow = PFS, red = PDMS, blue = PI).

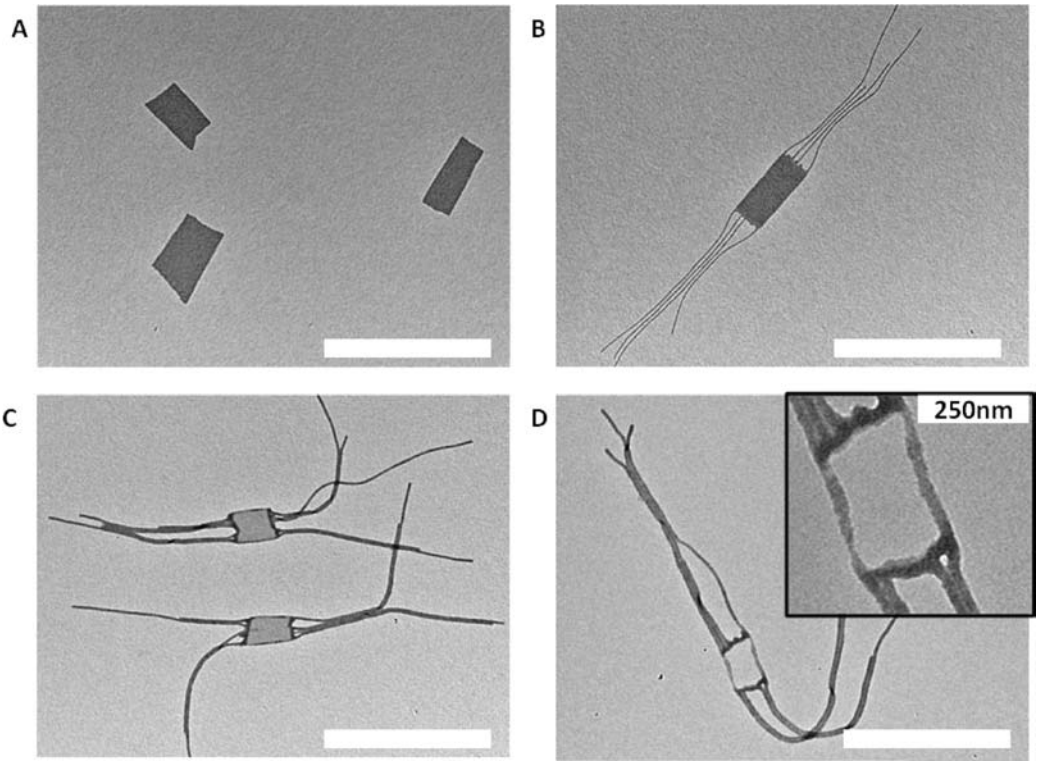

Figure 5. (A) PFS_{114}-*b*-$PDMS_{81}$ platelet micelles. (B) Scarf-like structures formed in the addition of PI_{637}-*b*-PFS_{53} to PFS_{114}-*b*-$PDMS_{81}$ platelet micelles. (C) Scarf-like structures after addition of 10 mol % Karstedt's catalyst. Darker regions are Pt(0) cross-linked PI_{637}-*b*-PFS_{53} domains. (D) Cross-linked scarf-like structures cast from THF. The hole in the middle of the structure corresponds to the non-cross-linkable PFS_{114}-*b*-$PDMS_{81}$ domain, which had previously dissolved in THF to leave behind only the cross-linked PI_{637}-*b*-PFS_{53} structure. Scale bars are 2000 nm unless noted otherwise.

showed that the PI corona regions of the micelles had been selectively darkened, while the PDMS corona regions remained unaffected (Figure 4B). When the pentablock comicelles were added to THF, the non-cross-linked PFS_{60}-*b*-$PDMS_{660}$ regions selectively dissolved to leave short, cross-linked PI_{637}-*b*-PFS_{53} micelles behind (Figure 4C). As before, adding dppe to the cross-linked pentablock micelles removed the Pt and the selective cross-linking/staining (Figure 4D).

Significantly, the staining of polyisoprene is not limited to PI-*b*-PFS block copolymers and was also successfully performed on PI-*b*-PEO spherical micelles. As with the PI-*b*-PFS cylindrical micelles, addition of Karstedt's catalyst to a decane solution of spherical PI_{514}-*b*-PEO_{250} micelles with a PEO core resulted in an increase of contrast in TEM micrographs due to Pt-coordination with the micelles (see Supporting Information, Figure S12a). Furthermore, the PI_{514}-*b*-PEO_{250} micelles were shown to be cross-linked, as they remained intact when drop-cast from a decane/THF 1:9 solution, a common solvent mixture for both blocks (see Supporting Information, Figure S12b).

3. Cross-Linking of Hierarchical Micelle Architectures. PFS BCPs with short corona-forming blocks self-assemble into

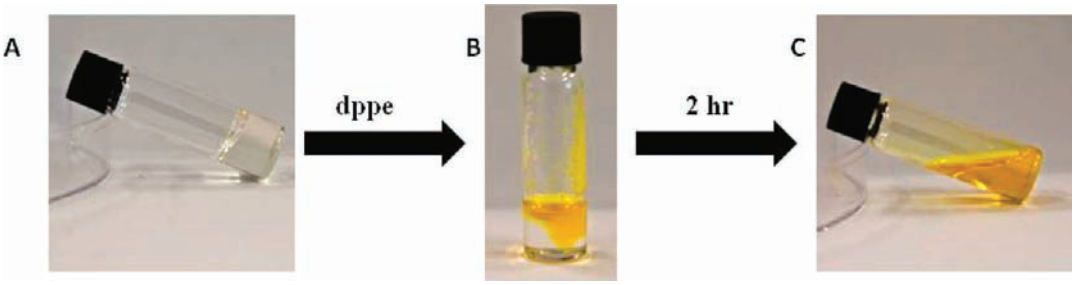

Figure 6. (A) 50 mg/mL PI_{2200} in a toluene/xylenes solution cross-linked with 5% Pt(0). (B) dppe added to the PI_{2200} polymer gel. In places where the dppe contacted the gel, a yellow color appeared due to the formation of $Pt(dppe)_2$. (C) 2 h after the addition of dppe to the gel, complete de-gelation had occurred.

lamellar-like platelet structures.[17] As with the cylindrical PFS BCP micelles, the PFS core of the platelets is crystalline and able to template the epitaxial crystallization-driven self-assembly of PFS BCP unimers. Thus, when cylinder-forming unimers are added to a solution of preformed PFS BCP platelets, cylindrical micelles preferentially develop at two edges of the platelets, resulting in complex structures with a scarf-like appearance.[19]

In order to demonstrate that the Pt(0) cross-linking method can be applied to more complex hierarchical micelle architectures, we first created PFS-*b*-PDMS platelets by dissolving PFS_{114}-*b*-$PDMS_{81}$ in a decane/xylene solution (9:1 v/v) (Scheme 3 and Figure 5A). Next, cylinder-forming PI_{637}-*b*-PFS_{53} unimers were added to the platelet solution to give PI_{637}-*b*-PFS_{53} tassels from the platelet edges (Scheme 3 and Figure 5B). As observed with the M(PFS-*b*-PDMS)-*b*-M(PI-*b*-PFS)-*b*-M(PFS-*b*-PDMS)-*b*-M(PI-*b*-PFS)-*b*-M(PFS-*b*-PDMS) pentablock micelles (Figure 4A), no discernible contrast was detected between the PI and PDMS corona domains of the scarf-like structures in the TEM micrographs (Figure 5B). However, upon addition of Karstedt's catalyst, the PI regions were selectively cross-linked and differentiable in TEM micrographs (Scheme 3 and Figure 5C). The selective staining of the polyisoprene revealed that a perimeter of PI_{637}-*b*-PFS_{53} had formed around the edge of the platelet in addition to the more noticeable cylindrical tassels (Scheme 3 and Figure 5C). Similar perimeter-forming behavior was observed when PI-*b*-PFG (PFG = polyferrocenyldimethylgermane) cylinders were grown from PI-*b*-PFS platelets.[19]

We were intrigued to explore whether the cross-linking of the PI-*b*-PFS cylinders and platelet perimeter should allow for the selective removal of the non-cross-linked PFS_{114}-*b*-$PDMS_{81}$ platelet while leaving the cross-linked connected PI-*b*-PFS domains intact. THF was added to a solution of platelets with cross-linked tassels, and then an aliquot was examined by TEM. As desired, the PFS-*b*-PDMS platelets dissolved away in the THF, leaving behind the PI-*b*-PFS tassels and platelet perimeter connected together via Pt(0) coordination cross-linking (Scheme 3 and Figure 5D). The TEM micrograph in Figure 5D shows a clear hole where the PDMS-*b*-PFS platelet previously existed. Overall, this demonstrated the successful use of PFS_{114}-*b*-$PDMS_{81}$ platelets to template the formation of the PI_{637}-*b*-PFS_{53} tassels, which upon Pt(0) cross-linking and subsequent addition of THF allowed for removal of the PFS_{114}-*b*-$PDMS_{81}$ to yield an unprecedented BCP self-assembled nanostructure.

4. Polyisoprene and Polybutadiene Gel Formation through Reversible Pt(0) Coordination. Although our interests were primarily concerned with the cross-linking of PI coronas in micellar structures, the ability of Karstedt's catalyst to coordinatively cross-link PI coronas should be transferable to PI and other diene homopolymers. Moreover, studies of the interaction of Pt(0) with homopolymer might be expected to provide further insight into the cross-linking mechanism with PI coronas. Reversible cross-linkable polymers are actively being developed as advanced materials for a wide array of applications.[39] To achieve reversible cross-linking, supramolecular interactions, including interchain hydrogen bonding[40] and metal ion coordination, are commonly employed.[41] Species containing thermodynamically reversible covalent bonds such as stable radical-forming alkoxyamines,[42] Diels–Alder cycloadducts,[43] and thiol-exchangeable disulfides[44] can also be used. In general, reversible cross-linkable polymers are often based around highly specialized, purposely designed polymers. Although PI is often cross-linked to improve its material properties, these processes are usually irreversible.[45] We are not aware of any other examples of reversible cross-linking of unmodified PI which leaves the polymer completely unaltered.

Table 2. Conditions Used To Form Polybutadiene Gels

entry	polymer	polymer concn (mg/mL)	Pt(0) mol %	gelation
1	1,2-PB_{1920}	50	1–5	yes
2	1,2-PB_{1920}	40	5	yes
3	1,2-PB_{1920}	30	5	yes
4	1,2-PB_{1920}	20	5	no
5	1,4-PB_{1840}	50	5	no

A toluene/xylenes solution consisting of 50 mg/mL PI_{2200} and 5 mol % (relative to the number of PI repeat units) of Karstedt's catalyst was found to form a gel upon standing (Figure 6A). Gel formation is strongly dependent on polymer concentration; we were unable to form gels with PI_{2200} concentrations lower than 50 mg/mL, although an increase in the viscosity of the solution was evident. When additional solvent was added to a preformed Pt(0)–PI_{2200} polymer, the polymer gel slowly dissolved, which is consistent with the dynamic reversibility of the Pt(0)–olefin coordination.

Solid dppe was added to the surface of a Pt(0)–PI_{2200} gel to assess the reversibility of the cross-linking. In regions where the surface of the gel came in contact with the dppe, the gel quickly turned yellow (Figure 6B). Over a period of 2 h, de-gelation occurred to form a bright yellow solution (Figure 6C); subsequent analysis by ^{31}P NMR spectroscopy showed the formation of $Pt(dppe)_2$. By ^{1}H NMR spectroscopy and GPC analysis, the PI_{2200} polymer was unaltered by the cross-linking process (see Supporting Information, Figures S13–S15).

The ability of dppe to reverse the cross-linking of a PI_{2200} gel formed from the Karstedt's catalyst-promoted hydrosilylation with TMDS was examined. First, 0.1 mol % Karstedt's catalyst and 1 mol % TMDS were added to a 50 mg/mL solution of PI_{2200} in toluene. After gelation occurred, dppe was added to the surface of the gel. The addition of dppe quickly caused the gel to turn bright yellow as the phosphine reacted with the platinum to form $Pt(dppe)_2$. However, unlike the gels formed using Karstedt's catalyst in isolation, the hydrosilylated gel was not disrupted since the phosphine is unable to disrupt the silicon−carbon bonds formed between TMDS and the polyisoprene vinyl groups. These results highlight a fundamental difference between the reversible coordination cross-linking of PI using Karstedt's catalyst alone and the irreversible hydrosilylation cross-linking of PI using TMDS in the presence of Karstedt's catalyst.

Adding Karstedt's catalyst to toluene solutions of 1,2-polybutadiene$_{1920}$ (1,2-PB_{1920}) also resulted in the formation of polymer gels. 1,2-PB_{1920} formed a gel with polymer concentrations as low as 30 mg/mL, much lower than the 50 mg/mL concentration needed with PI_{2200} (Table 2, entries 1−4). The difference likely arises due to the greater alkene/mass ratio and high vinyl content of 1,2-PB. Interestingly, 1,4-PB_{1840} did not form a gel under similar conditions with Karstedt's catalyst, although the solutions were noticeably more viscous upon the addition of the platinum complex (Table 2, entry 5). The lack of vinyl groups in 1,4-PB_{1840} compared to 1,2-PB_{1920} or PI_{2200} (PI_{2200} was polymerized anionically at −10 °C in THF and primarily has a 3,4/1,2 addition microstructure, see Chart 1)[45] could be responsible for the differences observed with 1,4-PB_{1840}.

We note that other examples of cross-linking polydienes by group 10 metals have been reported. Belfiore et al. showed that $PdCl_2(NCMe)_2$ cross-linked both 1,2-PB and 3,4/1,2-rich PI.[46] The authors proposed that the polymer alkene groups first displaced the acetonitrile ligands of $(CH_3CN)_2PdCl_2$, after which a Pd(II)-catalyzed coupling of alkene groups occurred.[46a] $PtCl_2(NCPh)_2$ was also shown to cross-link 1,2-PB, but at a much slower rate than the Pd(II) salt.[47] In all cases the cross-linking was not reversible and was unaffected by the addition of Ph_3P.[47] Thus, the Karstedt's catalyst-induced cross-linking of polyisoprene and polybutadiene reported in the present paper is clearly differentiated from the Pt(II) and Pd(II) cross-linking due to the ease with which the Pt(0) cross-linking is reversed with dppe.

SUMMARY

Karstedt's catalyst, acting as a source of Pt(0), was found to cross-link polyisoprene through alkene−Pt coordination. The Pt(0) cross-linking can be reversed through the addition of dppe, which as a bidentate phosphine is able to coordinate platinum to form $Pt(dppe)_2$. Analysis of ^1H NMR spectra and GPC traces of the PI-*b*-PFS block copolymer before and after removal of Pt(0) cross-linking by dppe showed no detectable change in polymer composition or size distribution.

Karstedt's catalyst can also be used as a selective TEM staining agent for PI coronas of PFS BCPs. The introduction of Pt(0) to the PI corona of PI-*b*-PFS micelles greatly increases the TEM contrast of the PI region. When applied to block micelles with distinct PI and PDMS corona blocks, only the PI was stained by platinum, allowing easy determination of micelle fine-structure. Compared to the difficult-to-handle and toxic OsO_4, Karstedt's catalyst is much safer to work with and can be delivered in precise amounts to micelle solutions for selective staining purposes.

Pt(0) cross-linking of PI can be employed in the preparation of complex hierarchical structures. Using a PFS-*b*-PDMS platelet micelle as a template, PI-*b*-PFS tassels were grown to form a scarf-shaped structure. Karstedt's catalyst was first used to cross-link the PI corona domains, after which the PFS-*b*-PDMS template was removed using THF, a common solvent for PFS and PDMS. After PFS-*b*-PDMS removal, a hollowed-out PI-*b*-PFS structure remained, held together by the Pt(0)−alkene coordination within the PI corona.

Reversible cross-linking of polyisoprene with Karstedt's catalyst is not limited to BCP micelles and can be used to form gels of PI homopolymer. As with the micellar systems, the cross-linking was reversed by adding dppe, leaving the PI chemically unaltered by the process. 1,2-PB behaved comparably to PI and was able to form gels in the presence of Pt(0). Interestingly, 1,4-PB did not gel under similar conditions, probably due to the lack of vinyl groups compared to 1,2-PB or 1,2/3,4-rich PI. Presumably, Pt(0) can bind more strongly to vinyl groups than to the more substituted alkene groups of 1,4-PB.

We have presented a facile method for the reversible cross-linking of polyisoprene and polybutadiene. Since the cross-linking of polydienes can be used to generate BCP micelles with a variety of complex morphologies,[48] we expect this methodology to open up new opportunities in the field of BCP self-assembly. For example, the use of reversible Pt(0) cross-linking may present advantages similar to the use of protecting groups in organic synthesis. Thus, reversible Pt(0) cross-linking could be utilized to temporarily increase the structural integrity of a polydiene BCP micelle during the course of a physical or chemical transformation which, in the absence of cross-linking, would disrupt the self-assembly. Afterward, the cross-links could be removed, and the polydiene block would be left unaltered and available for further functionalization.[49] The embedding of Pt(0) centers into polydiene coronas may also impart useful catalytic properties. Furthermore other, less expensive transition metals capable of forming metal−olefin bonds may also reversibly cross-link polydienes. Relevant studies based on all of the aforementioned concepts are in progress.

ASSOCIATED CONTENT

Supporting Information. Experimental procedures, EDX spectra, TEM micrographs, GPC chromatograms, and ^1H and ^{31}P NMR spectrographs. This material is available free of charge via the Internet at http://pubs.acs.org.

AUTHOR INFORMATION

Corresponding Author
mwinnik@chem.utoronto.ca; ian.manners@bristol.ac.uk

ACKNOWLEDGMENT

P.A.R. is grateful to the NSERC of Canada for an NSERC Postdoctoral Fellowship and the EU for a Marie Curie Fellowship. I.M. thanks the European Union for a Marie Curie Chair, a Reintegration Grant, and an Advanced Investigator Grant and also the Royal Society for a Wolfson Research Merit Award. M.A.W. thanks the NSERC of Canada for financial support. The authors also thank Dr. Torben Gädt for synthesizing PFS_{28}-*b*-$PDMS_{560}$.

REFERENCES

(1) (a) Rodríguez-Hernández, J.; Chécot, F.; Gnanou, Y.; Lecommandoux, S. *Prog. Polym. Sci.* **2005**, *30*, 691. (b) Riess, G. *Prog. Polym. Sci.* **2003**, *28*, 1107. (c) Gohy, J. F. *Coord. Chem. Rev.* **2009**, *253*, 2214.

(2) (a) Schleuss, T. W.; Abbel, R.; Gross, M.; Schollmeyer, D.; Frey, H.; Maskos, M.; Berger, R.; Kilbinger, A. F. M. *Angew. Chem., Int. Ed.* **2006**, *45*, 2969. (b) Pochan, D. J.; Chen, Z. Y.; Cui, H. G.; Hales, K.; Qi, K.; Wooley, K. L. *Science* **2004**, *306*, 94. (c) Li, Z. B.; Kesselman, E.; Talmon, Y.; Hillmyer, M. A.; Lodge, T. P. *Science* **2004**, *306*, 98. (d) Li, Z. B.; Chen, Z. Y.; Cui, H. G.; Hales, K.; Qi, K.; Wooley, K. L.; Pochan, D. J. *Langmuir* **2005**, *21*, 7533. (e) Dupont, J.; Liu, G.; Niihara, K.-i.; Kimoto, R.; Jinnai, H. *Angew. Chem., Int. Ed.* **2009**, *48*, 6144. (f) Fang, B.; Walther, A.; Wolf, A.; Xu, Y.; Yuan, J.; Müller, A. H. E. *Angew. Chem., Int. Ed.* **2009**, *48*, 2877. (g) Schacher, F.; Walther, A.; Ruppel, M.; Drechsler, M.; Müller, A. H. E. *Macromolecules* **2009**, *42*, 3540. (h) Discher, D. E.; Eisenberg, A. *Science* **2002**, *297*, 967.

(3) (a) Kedar, U.; Phutane, P.; Shidhaye, S.; Kadam, V. *Nanomed. Nanotechnol. Biol. Med.* **2010**, *6*, 714. (b) Sun, H. L.; Guo, B. N.; Cheng, R.; Meng, F. H.; Liu, H. Y.; Zhong, Z. Y. *Biomaterials* **2009**, *30*, 6358. (c) Ren, T. B.; Feng, Y.; Zhang, Z. H.; Li, L.; Li, Y. Y. *Soft Matter* **2011**, *7*, 2329. (d) Lee, S. J.; Min, K. H.; Lee, H. J.; Koo, A. N.; Rim, H. P.; Jeon, B. J.; Jeong, S. Y.; Heo, J. S.; Lee, S. C. *Biomacromolecules* **2011**, *12*, 1224.

(4) Cao, L.; Massey, J. A.; Winnik, M. A.; Manners, I.; Riethmüller, S.; Banhart, F.; Spatz, J. P.; Möller, M. *Adv. Funct. Mater.* **2003**, *13*, 271.

(5) (a) Spatz, J. P.; Mossmer, S.; Hartmann, C.; Möller, M.; Herzog, T.; Krieger, M.; Boyen, H. G.; Ziemann, P.; Kabius, B. *Langmuir* **2000**, *16*, 407. (b) Lohmueller, T.; Bock, E.; Spatz, J. P. *Adv. Mater.* **2008**, *20*, 2297. (c) Koh, H.-D.; Park, S.; Russell, T. P. *ACS Nano* **2010**, *4*, 1124. (d) Khanal, A.; Inoue, Y.; Yada, M.; Nakashima, K. *J. Am. Chem. Soc.* **2007**, *129*, 1534.

(6) Matsumoto, K.; Matsuoka, H. *J. Polym. Sci., Polym. Chem.* **2005**, *43*, 3778.

(7) Thio, Y. S.; Wu, J.; Bates, F. S. *Macromolecules* **2006**, *39*, 7187.

(8) (a) Thurmond, K. B.; Kowalewski, T.; Wooley, K. L. *J. Am. Chem. Soc.* **1996**, *118*, 7239. (b) Huang, H. Y.; Kowalewski, T.; Remsen, E. E.; Gertzmann, R.; Wooley, K. L. *J. Am. Chem. Soc.* **1997**, *119*, 11653. (c) Guo, A.; Liu, G.; Tao, J. *Macromolecules* **1996**, *29*, 2487. (d) Ding, J. F.; Liu, G. J. *Macromolecules* **1998**, *31*, 6554.

(9) (a) Read, E. S.; Armes, S. P. *Chem. Commun.* **2007**, 3021. (b) O'Reilly, R. K.; Hawker, C. J.; Wooley, K. L. *Chem. Soc. Rev.* **2006**, *35*, 1068. (c) van Nostrum, C. F. *Soft Matter* **2011**, *7*, 3246.

(10) (a) Thurmond, K. B.; Kowalewski, T.; Wooley, K. L. *J. Am. Chem. Soc.* **1997**, *119*, 6656. (b) Prochazka, K.; Baloch, M. K.; Tuzar, Z. *Makromol. Chem.* **1979**, *180*, 2521. (c) Iijima, M.; Nagasaki, Y.; Okada, T.; Kato, M.; Kataoka, K. *Macromolecules* **1999**, *32*, 1140. (d) Huang, H. Y.; Hoogenboom, R.; Leenen, M. A. M.; Guillet, P.; Jonas, A. M.; Schubert, U. S.; Gohy, J. F. *J. Am. Chem. Soc.* **2006**, *128*, 3784. (e) Cao, L.; Manners, I.; Winnik, M. A. *Macromolecules* **2001**, *34*, 3353.

(11) (a) Yusa, S.; Sugahara, M.; Endo, T.; Morishima, Y. *Langmuir* **2009**, *25*, 5258. (b) Shi, D. J.; Matsusaki, M.; Akashi, M. *Bioconjugate Chem.* **2009**, *20*, 1917. (c) Saito, K.; Ingalls, L. R.; Lee, J.; Warner, J. C. *Chem. Commun.* **2007**, 2503. (d) Jamroz-Piegza, M.; Walach, W.; Dworak, A.; Trzebicka, B. *J. Colloid Interface Sci.* **2008**, *325*, 141. (e) He, J.; Tong, X.; Zhao, Y. *Macromolecules* **2009**, *42*, 4845. (f) Hoppenbrouwers, E.; Li, Z.; Liu, G. J. *Macromolecules* **2003**, *36*, 876. (g) Li, Z.; Liu, G. J. *Langmuir* **2003**, *19*, 10480. (h) Liu, F. T.; Liu, G. J. *Macromolecules* **2001**, *34*, 1302.

(12) (a) Yang, Z.; Zheng, S. Y.; Harrison, W. J.; Harder, J.; Wen, X. X.; Gelovani, J. G.; Qiao, A.; Li, C. *Biomacromolecules* **2007**, *8*, 3422. (b) Wei, H.; Wu, D. Q.; Li, Q.; Chang, C.; Zhou, J. P.; Zhang, X. Z.; Zhuo, R. X. *J. Phys. Chem. C* **2008**, *112*, 15329. (c) Wei, H.; Cheng, C.; Chang, C.; Chen, W. Q.; Cheng, S.; Zhang, X. Z.; Zhuo, R. X. *Langmuir* **2008**, *24*, 4564. (d) Du, J. Z.; Chen, Y. M.; Zhang, Y. H.; Han, C. C.; Fischer, K.; Schmidt, M. *J. Am. Chem. Soc.* **2003**, *125*, 14710. (e) Du, J. Z.; Chen, Y. M. *Macromol. Rapid Commun.* **2005**, *26*, 491. (f) Du, J. Z.; Armes, S. P. *J. Am. Chem. Soc.* **2005**, *127*, 12800. (g) Chang, C.; Wei, H.; Feng, J.; Wang, Z. C.; Wu, X. J.; Wu, D. Q.; Cheng, S. X.; Zhang, X. Z.; Zhuo, R. X. *Macromolecules* **2009**, *42*, 4838.

(13) (a) Rodriguez-Hernandez, J.; Babin, J.; Zappone, B.; Lecommandoux, S. *Biomacromolecules* **2005**, *6*, 2213. (b) Remsen, E. E.; Thurmond, K. B.; Wooley, K. L. *Macromolecules* **1999**, *32*, 3685. (c) O'Reilly, R. K.; Joralemon, M. J.; Hawker, C. J.; Wooley, K. L. *J. Polym. Sci., Polym. Chem.* **2006**, *44*, 5203. (d) Liu, S. Y.; Ma, Y. H.; Armes, S. P. *Langmuir* **2002**, *18*, 7780. (e) Bütün, V.; Lowe, A. B.; Billingham, N. C.; Armes, S. P. *J. Am. Chem. Soc.* **1999**, *121*, 4288. (f) Bütün, V.; Billingham, N. C.; Armes, S. P. *J. Am. Chem. Soc.* **1998**, *120*, 12135.

(14) Meng, F. H.; Hennink, W. E.; Zhong, Z. *Biomaterials* **2009**, *30*, 2180.

(15) Whittell, G. R.; Hager, M. D.; Schubert, U. S.; Manners, I. *Nat. Mater.* **2011**, *10*, 176.

(16) (a) Massey, J. A.; Temple, K.; Cao, L.; Rharbi, Y.; Raez, J.; Winnik, M. A.; Manners, I. *J. Am. Chem. Soc.* **2000**, *122*, 11577. (b) Massey, J.; Power, K. N.; Manners, I.; Winnik, M. A. *J. Am. Chem. Soc.* **1998**, *120*, 9533.

(17) Cao, L.; Manners, I.; Winnik, M. A. *Macromolecules* **2002**, *35*, 8258.

(18) Wang, X. S.; Guerin, G.; Wang, H.; Wang, Y. S.; Manners, I.; Winnik, M. A. *Science* **2007**, *317*, 644.

(19) Gädt, T.; Ieong, N. S.; Cambridge, G.; Winnik, M. A.; Manners, I. *Nat. Mater.* **2009**, *8*, 144.

(20) Gilroy, J. B.; Gädt, T.; Whittell, G. R.; Chabanne, L.; Mitchels, J. M.; Richardson, R. M.; Winnik, M. A.; Manners, I. *Nat. Chem.* **2010**, *2*, 566.

(21) Gädt, T.; Schacher, F. H.; McGrath, N.; Winnik, M. A.; Manners, I. *Macromolecules* **2011**, *44*, 3777.

(22) Petzetakis, N.; Dove, A. P.; O'Reilly, R. K. *Chem. Sci.* **2011**, *2*, 955.

(23) Patra, S. K.; Ahmed, R.; Whittell, G. R.; Lunn, D. J.; Dunphy, E. L.; Winnik, M. A.; Manners, I. *J. Am. Chem. Soc.* **2011**, *133*, 8842.

(24) (a) Wang, X.-S.; Winnik, M. A.; Manners, I. *Angew. Chem., Int. Ed.* **2004**, *43*, 3703. (b) Wang, X.-S.; Wang, H.; Coombs, N.; Winnik, M. A.; Manners, I. *J. Am. Chem. Soc.* **2005**, *127*, 8924. (c) Wang, X.-S.; Arsenault, A.; Ozin, G. A.; Winnik, M. A.; Manners, I. *J. Am. Chem. Soc.* **2003**, *125*, 12686. (d) Wang, X. S.; Liu, K.; Arsenault, A. C.; Rider, D. A.; Ozin, G. A.; Winnik, M. A.; Manners, I. *J. Am. Chem. Soc.* **2007**, *129*, 5630.

(25) Karstedt, B. D. U.S. Patent 3775452, 1973.

(26) Lewis, L. N.; Stein, J.; Gao, Y.; Colborn, R. E.; Hutchins, G. *Plat. Met. Rev.* **1997**, *41*, 66.

(27) (a) Lappert, M. F.; Scott, F. P. A. *J. Organomet. Chem.* **1995**, *492*, C11. (b) Stein, J.; Lewis, L. N.; Gao, Y.; Scott, R. A. *J. Am. Chem. Soc.* **1999**, *121*, 3693. (c) Hitchcock, P. B.; Lappert, M. F.; Warhurst, N. J. W. *Angew. Chem., Int. Ed.* **1991**, *30*, 438.

(28) Green, M.; Howard, J. A. K.; Spencer, J. L.; Stone, F. G. A. *J. Chem. Soc., Dalton Trans.* **1977**, 271.

(29) (a) Guérin, G. r.; Wang, H.; Manners, I.; Winnik, M. A. *J. Am. Chem. Soc.* **2008**, *130*, 14763. (b) Qian, J.; Guerin, G.; Cambridge, G.; Manners, I.; Winnik, M. A. *Macromol. Rapid Commun.* **2010**, *31*, 928.

(30) Qian, J. S.; Guerin, G.; Lu, Y. J.; Cambridge, G.; Manners, I.; Winnik, M. A. *Angew. Chem., Int. Ed.* **2011**, *50*, 1622.

(31) Sivaramakrishna, A.; Clayton, H. S.; Mogorosi, M. M.; Moss, J. R. *Coord. Chem. Rev.* **2010**, *254*, 2904.

(32) (a) Krause, J.; Cestaric, G.; Haack, K.-J.; Seevogel, K.; Storm, W.; Pörschke, K.-R. *J. Am. Chem. Soc.* **1999**, *121*, 9807. (b) Berthon-Gelloz, G.; Schumers, J.-M.; Lucaccioni, F.; Tinant, B.; Wouters, J.; Markó, I. E. *Organometallics* **2007**, *26*, 5731.

(33) Chandra, G.; Lo, P. Y.; Hitchcock, P. B.; Lappert, M. F. *Organometallics* **1987**, *6*, 191.

(34) Clark, H. C.; Kapoor, P. N.; McMahon, I. J. *J. Organomet. Chem.* **1984**, *265*, 107.

(35) Lewis, L. N.; Colborn, R. E.; Grade, H.; Bryant, G. L.; Sumpter, C. A.; Scott, R. A. *Organometallics* **1995**, *14*, 2202.

(36) Smith, A. E.; Xu, X.; Savin, D. A.; McCormick, C. L. *Poly. Chem.* **2010**, *1*, 628.

(37) Preliminary experiments have shown that when TMDS is added to PI-*b*-PFS micelles with Pt(0)-induced cross-linking, the Pt(0) embedded in the PI corona is still capable of catalyzing the hydrosilylation reaction.

(38) Sawyer, L. C.; Grubb, D. T.; Meyers, G. F. *Polymer Microscopy*; Springer: New York, 2008.

(39) (a) Wojtecki, R. J.; Meador, M. A.; Rowan, S. J. *Nat. Mater.* **2011**, *10*, 14. (b) Kloxin, C. J.; Scott, T. F.; Adzima, B. J.; Bowman, C. N. *Macromolecules* **2010**, *43*, 2643.

(40) (a) Nair, K. P.; Breedveld, V.; Weck, M. *Macromolecules* **2008**, *41*, 3429. (b) Nair, K. P.; Breedveld, V.; Weck, M. *Soft Matter* **2011**, *7*, 553. (c) Nair, K. P.; Weck, M. *Macromolecules* **2006**, *40*, 211.

(41) (a) Kersey, F. R.; Loveless, D. M.; Craig, S. L. *J. R. Soc. Interface* **2007**, *4*, 373. (b) Pollino, J. M.; Nair, K. P.; Stubbs, L. P.; Adams, J.; Weck, M. *Tetrahedron* **2004**, *60*, 7205. (c) Paulusse, J. M. J.; van Beek, D. J. M.; Sijbesma, R. P. *J. Am. Chem. Soc.* **2007**, *129*, 2392. (d) Yuan, X.; Shen, F.; Wu, G.; Wu, C. *Polym. Compos.* **2008**, *29*, 302.

(42) Higaki, Y.; Otsuka, H.; Takahara, A. *Macromolecules* **2006**, *39*, 2121.

(43) Chen, X.; Dam, M. A.; Ono, K.; Mal, A.; Shen, H.; Nutt, S. R.; Sheran, K.; Wudl, F. *Science* **2002**, *295*, 1698.

(44) Chong, S. F.; Chandrawati, R.; Stadler, B.; Park, J.; Cho, J. H.; Wang, Y. J.; Jia, Z. F.; Bulmus, V.; Davis, T. P.; Zelikin, A. N.; Caruso, F. *Small* **2009**, *5*, 2601.

(45) Odian, G. *Principles of Polymerization*, 4th ed.; Wiley -Interscience: Hoboken, NJ, 2004.

(46) (a) Bosse, F.; Das, P.; Belfiore, L. A. *Macromolecules* **1995**, *28*, 6993. (b) Bosse, F.; Das, P.; Belfiore, L. A. *J. Polym. Sci. B, Polym. Phys.* **1996**, *34*, 909. (c) Bosse, F.; Das, P.; Belfiore, L. A. *Polym. Gels Netw.* **1997**, *5*, 387.

(47) Belfiore, L. A.; Das, P. K. *J. Polym. Sci. B, Polym. Phys.* **2004**, *42*, 2270.

(48) (a) Yelamanchili, R. S.; Walther, A.; Müller, A. H. E.; Breu, J. *Chem. Commun.* **2008**, 489. (b) Walther, A.; Drechsler, M.; Rosenfeldt, S.; Harnau, L.; Ballauff, M.; Abetz, V.; Müller, A. H. E. *J. Am. Chem. Soc.* **2009**, *131*, 4720.

(49) (a) Korthals, B.; Morant-Minana, M. C.; Schmid, M.; Mecking, S. *Macromolecules* **2010**, *43*, 8071. (b) ten Brummelhuis, N.; Diehl, C.; Schlaad, H. *Macromolecules* **2008**, *41*, 9946. (c) Hoyle, C. E.; Bowman, C. N. *Angew. Chem., Int. Ed.* **2010**, *49*, 1540.